Lightning Observations in Northern Colorado Snowstorms

Matthew R. Kumjian[1,*] and Wiebke Deierling[2]

1. Pennsylvania State University, State College, PA, United States
2. National Center for Atmospheric Research, Boulder, CO, United States

ABSTRACT: Lightning flashes during snowstorms occur infrequently compared to warm-season convective storms. The rarity of such events may pose an additional hazard because of their unexpected nature. In addition, because cloud electrification in thundersnow events leads to only few lightning discharges, studying thundersnow events may offer additional insights into mechanisms for charging and possible thresholds required for lightning discharges.

In this study, we present observations of four Northern Colorado thundersnow events that occurred in the 2012-2013 winter season. Detailed total lightning information was collected by the Colorado Lightning Mapping Array allowing for the analysis of lightning characteristics and storm charge structure of these cases. Lightning data from CONUS lightning detection networks are also examined. Dual-polarization radar data from the WSR-88D radars near Denver (KFTG) and Cheyenne (KCYS) are analyzed to uncover the microphysical structure of the lightning-producing storms. The occurrence of four thundersnow events in one season strongly disagrees with previous climatologies, implying that thundersnow may be more common than previously thought.

Most of the lightning flashes occurred within convective cells, in which polarimetric radar data reveal the collocation of graupel and pristine ice crystals. However, some flashes occurred in snow bands lacking any apparent convective structure. In some of these cases, depolarization streaks were observed in the radar data, indicating sufficiently strong electric fields as to orient pristine ice crystals. In several cases, flashes occurred in cells that were located over the Palmer Divide, a topographic feature that may have enhanced updrafts. Similarities among the different cases are described.

INTRODUCTION

Thundersnow events are rare phenomena and are defined as snow-bearing storms that produce lightning and thunder. Because lightning in winter storms may seem counterintuitive and is rare, such events may take forecasters and the public by surprise and may pose an unexpected hazard. Thus, better understanding of these unique storms could serve to mitigate potential risks.

Schultz and Vavrek (2009) provide a good review of historical observations of thundersnow events, which are limited because of their extreme rarity. For example, Curran and Pearson (1971) investigated 76

* Contact information: Matthew Kumjian, Pennsylvania State University, 513 Walker Building, University Park, PA, United States, Email: kumjian@psu.edu

thundersnow cases in the United States and found that only 1.3% of cool-season thunderstorms (i.e., those occurring between October and May) produced snow, and that only 0.07% of snowfall observations were associated with lightning or thunder. Further, the climatology by Market et al. (2002) reported only 3 incidences of thundersnow in Northern Colorado over a 30-year period from 1961-1990, with an average annual occurrence of only 6.3 events in the entire contiguous United States.

As pointed out in Schultz and Vavrek (2009), the same ingredients needed for warm-season thunderstorms must be present in thundersnow events: moisture, lift, and an unstable temperature profile. Curran and Pearson (1971) showed that the mean environment of their thundersnow cases was supportive of elevated convection, with a stable boundary layer topped by a near-neutral thermal profile. Market et al. (2006) found similar results for thundersnow events in the central United States, with the most unstable level roughly 30 to 50 hPa above the top of the low-level temperature inversion. In addition, cold (< 0 °C) air is required to produce snow at the surface. The composite sounding in Market et al. (2006) was cold enough throughout the layer to support snow. The surface temperature often is found to be very near 0 °C (e.g., Schultz 1999; Hunter et al. 2001; Stuart 2001). Market et al. (2002) found the mean surface temperature in their thundersnow cases to be about -1 °C.

Several authors have also investigated thundersnow events using radar. A series of studies of an electrified storm over the Sea of Japan made use of C-band dual-polarization radar data (Fukao et al. 1991; Maekawa et al. 1992, 1993). These authors noted the collocation of radar-inferred graupel and ice crystals at the -10 °C level preceding lightning flashes. They also found that the lightning-producing cell exhibited $Z_H > 40$ dBz, whereas other nearby cells did not. The lightning production seemed to be tied to an increase in the inferred graupel content. Pettegrew et al. (2009) used data from a single-polarization WSR-88D radar to investigate a thundersnow event over eastern Iowa and north-central Illinois. The echo top of the storm in their case study never exceeded about 3.7 km AGL, and its maximum reflectivity values never surpassed 40 – 45 dBz. These maximum reflectivity values were confined to the lowest levels.

The documentation of thundersnow events has been rare. In the United States most observations have been from national lightning detection networks that mostly detect cloud-to-ground lightning, which only comprise a fraction of all lightning discharges (Boccippio et al. 2001). However, with the growing availability of regional total lightning detection systems such as the Lightning Mapping Array (LMA) systems developed by the New Mexico Institute of Mining and Technology (NMIMT) that detect both cloud-to-ground (CG) and in-cloud (IC) flashes with high detection efficiency and accuracy (Thomas et al. 2004, Lang et al. 2004) within a 100 - 200 km range, it is possible to document events that previously may have gone undetected. We are investigating 4 events that occurred in Northern Colorado over a 5.5-month period in the 2012-2013 cold season. Though unclear whether the 2012-2013 season was anomalous, it does hint at the possibility that thundersnow events are far more common than previously documented.

In addition to the Colorado LMA (COLMA), all of the Weather Surveillance Radar 1988 Doppler (WSR-88D) radars in the region were recently upgraded to have dual-polarization capabilities. The added information available from the polarimetric radar variables could provide further insight into the microphysical structure of these thundersnow storms. The next section provides an overview of the instrumentation and data used to analyze these thundersnow events in this study. The following section presents an overview the cases and some results of the data analysis, followed by a discussion and

summary of the main conclusions.

INSTRUMENTATION AND DATA

The National Weather Service WSR-88D radar network recently has undergone an upgrade to have dual-polarization capabilities. In addition to the conventional moments of reflectivity factor at horizontal polarization (Z_H), Doppler velocity (V_r), and Doppler spectrum width (σ_w), the polarimetric radars provide the differential reflectivity (Z_{DR}), differential propagation phase (Φ_{DP}), and the co-polar correlation coefficient (ρ_{hv} or CC). Descriptions of these polarimetric variables and their informative content can be found in Doviak and Zrnić (1993), Zrnić and Ryzhkov (1999), Straka et al. (2000), Bringi and Chandrasekar (2001), Ryzhkov et al. (2005), and Kumjian (2013a,b,c), among others.

So-called "level-II" radar data from the WSR-88D polarimetric (hereafter WSR-88DP) radars near Denver (KFTG) and Cheyenne (KCYS) are used in this study. In addition to the level-II base variables, the output of the operational hydrometeor classification algorithm (HCA) is used. The current HCA combines the informative contents of each polarimetric radar variable and determines the scatterer dominating the returned signals in each radar sampling volume (Park et al. 2009). Currently, one of 10 possible classes is assigned: Light-to-moderate rain, heavy rain, "big drops", rain mixed with hail, graupel, wet snow, dry snow aggregates, ice crystals, biological scatterers, and ground clutter and/or anomalous propagation.

Three dimensional total lighting data collected by COLMA was used in this study to document the total flash rate from the thundersnow events as well as deduce the location and polarity of charge layers within storm cells. The COLMA consists of 15 stations and is a time of arrival system that detects the three-dimensional positions (x, y, z coordinates) of VHF sources emitted from lightning discharges at around 60 – 66 MHz (Thomas et al. 2004).

OVERVIEW OF EVENTS

Four thundersnow cases were observed in Northern Colorado in the 2012/2013 cold season. The synoptic conditions for each thundersnow case reveal similarities (Fig. 1). In 11 November, 28 January, and 9 April, a large-scale positively-tilted trough is located to the west of Colorado, over the Rocky Mountains. On 25 October, the trough axis has just passed through Colorado and is lifting out. A ridge is located over the eastern United States in all four cases. In each case, a surface low is located to the south or east of the COLMA domain, and a cold frontal passage has just occurred, with surface temperatures very near 0 °C. The surface features provide northerly or northeasterly upslope flow, overlaid by larger-scale southwesterly flow aloft. The proximity of the upper-level trough would support large-scale ascent across the region.

The analysis domain is shown in Figure 2. Locations of the LMA sources from each case are overlaid, as are the locations of the COLMA stations, the WSR-88DP radar near Denver (KFTG), and the National Weather Service Denver sounding site (DNR). One immediately sees a preferred location for lightning activity south of the LMA network, seemingly anchored to the terrain feature known as the Palmer Divide. The northerly or northeasterly upslope low-level flow in each case would favor enhanced uplift at the Palmer Divide. Such enhanced rising motion plausibly could provide an extra boost to storms, favoring otherwise marginal storms for updrafts sufficiently strong as to promote electrification.

Other features of note in Figure 2 include linear tracks of static discharges seen by the LMA that are produced by aircraft departing from or arriving at Denver International Airport. The LMA sees sparks that are caused by aircrafts that get charged up (through collisional charging of the aircrafts fuselage with ice particles) when flying through ice clouds (e.g. Thomas et al. 2004).

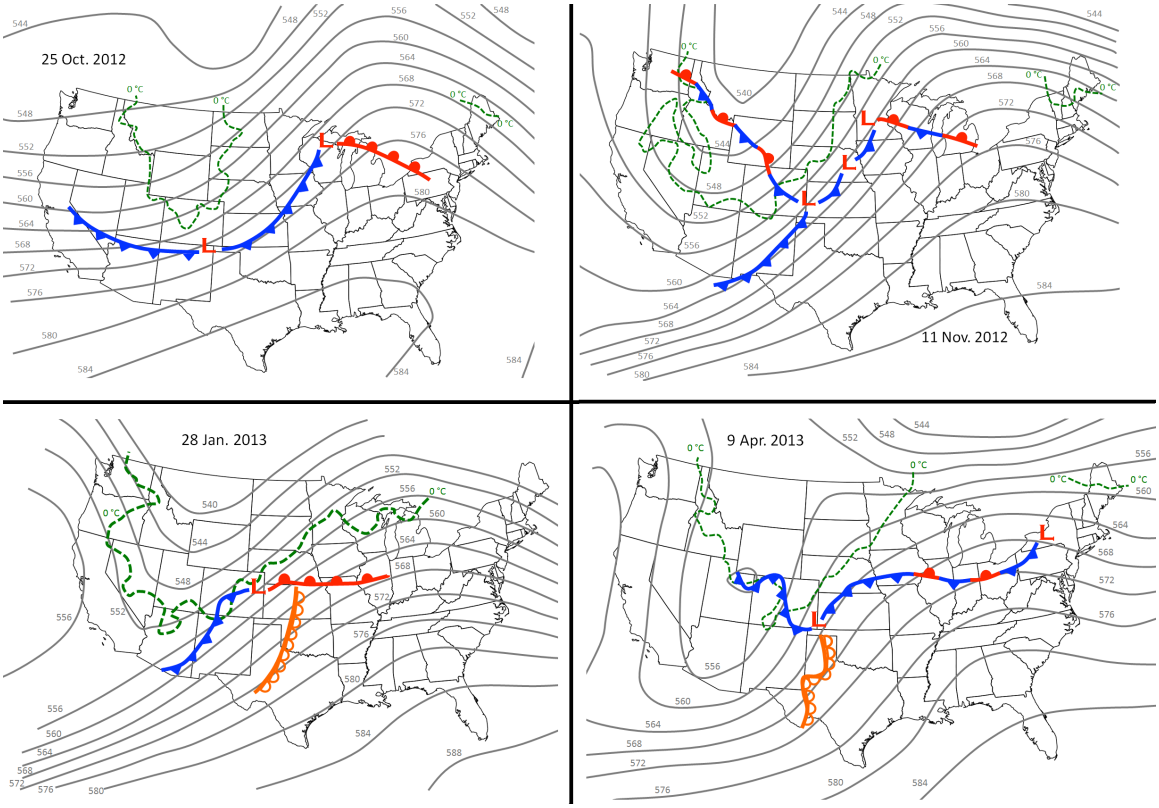

Figure 1: *Synoptic overview of each thundersnow case. In each panel, 500 hPa heights (in dkm) are shown in gray curves, overlaid by selected surface features including the 0 °C isotherm (dashed green line), location of surface low pressure centers, and surface fronts. Analyses are adopted from the NCEP HPC. Upper-air (surface) analyses are valid for (a) 25 October 2012 at 0000 (0300) UTC, (b) 11 November 2012 at 0000 (0000) UTC, (c) 29 (28) January 2013 at 0000 (2100) UTC, and (d) 9 April 2013 at 1200 (0700) UTC.*

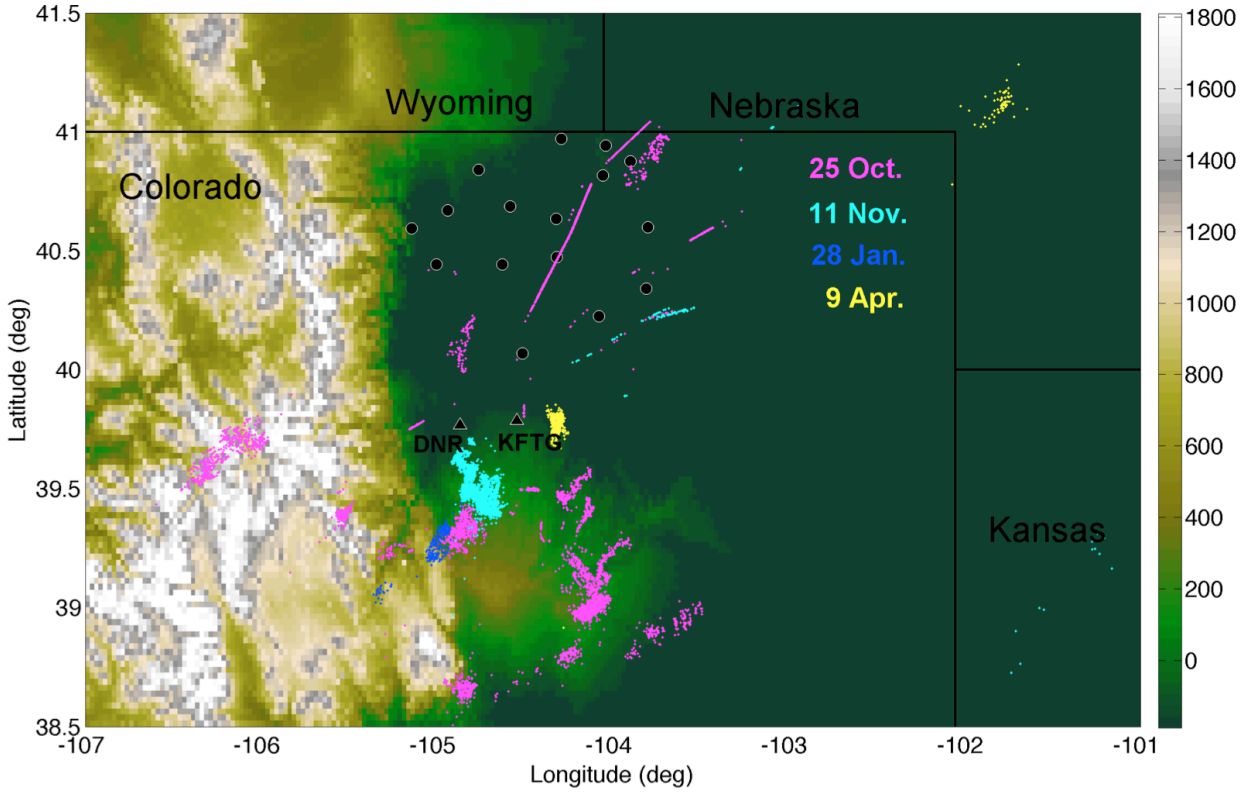

Figure 2: *Map of terrain (in meters above DNR site) in the study domain. Locations of sounding (DNR) and radar (KFTG) sites shown by triangle markers. Colorado LMA stations given in black circle markers. Pink dots represent LMA sources from 25 October 2012; cyan dots represent source points for 11 November 2012; blue points for 28 January 2013; yellow points for 9 April 2013.*

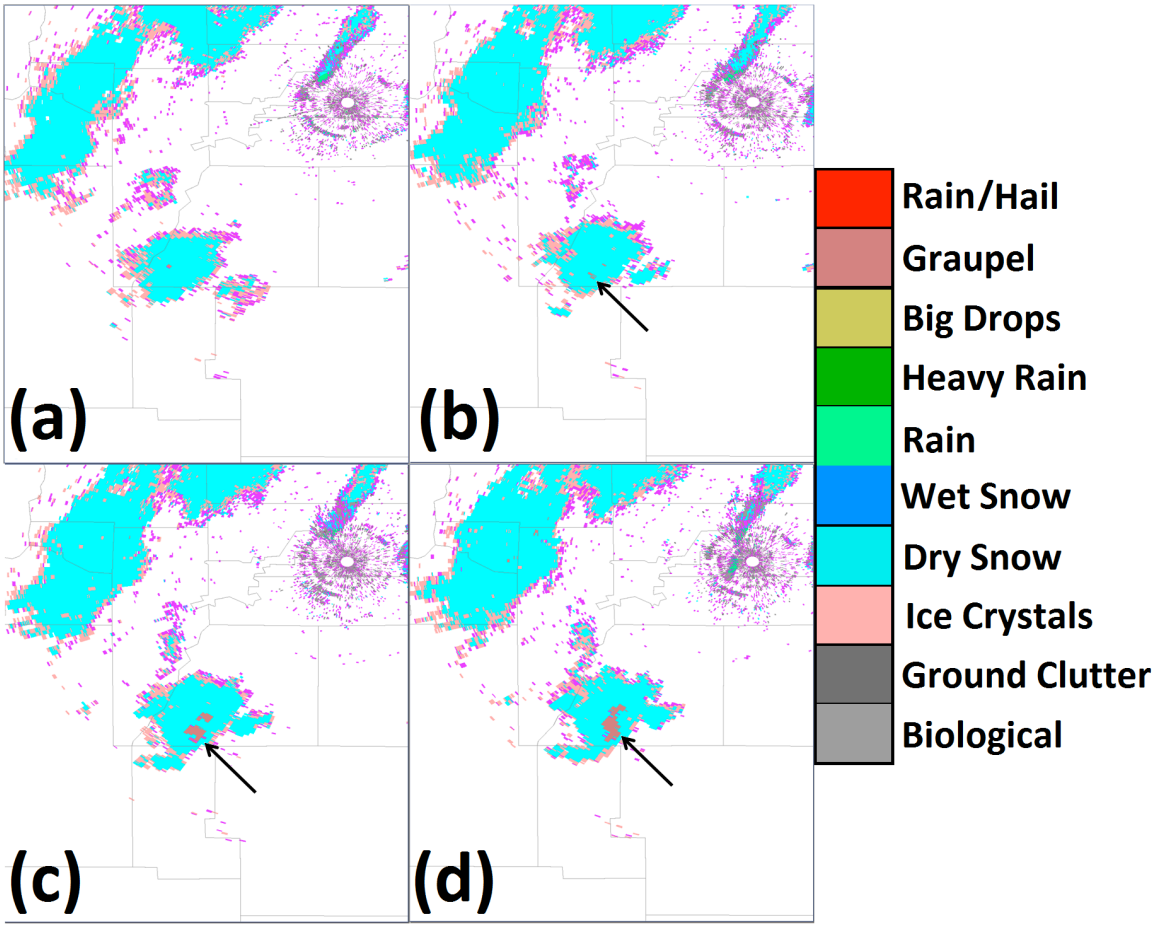

Figure 3: *KFTG 2.4 deg scans showing the operational hydrometeor classification algorithm output for 4 consecutive scans (a) 2124:17 UTC, (b) 2131:03 UTC, (c) 2135:43 UTC, and (d) 2140:25 UTC on 28 January 2013. Arrows indicate the regions classified as graupel (salmon color).*

The upgraded WSR-88DP radar network employs a hydrometeor classification algorithm (HCA; Park et al. 2009) that classifies each radar pixel as one of 10 possible classes: biological scatterers, ground clutter / anomalous propagation, pristine ice crystals, dry snow aggregates, wet snow, light-to-moderate rain, heavy rain, "big drops", graupel, and a mixture of rain and hail. Figure 3 provides the evolution of the HCA output at the 2.4° elevation angle from 2124:17 through 2140:25 UTC during the 28 January 2013 case. Initially, mainly dry snow aggregates are classified in the cell to the southwest of the radar (Figure 3a). By the 2131:03 scan (Figure 3b), a few contiguous pixels of graupel are identified. This region expands considerably in the next two scans (Figures. 3 c-d). Such a rapid appearance and expansion of graupel identifications is suggestive of convective activity and considerable ongoing riming within a region of snow aggregates and ice crystals, which are precursors to electrification. The first LMA sources occurred shortly after 2140 UTC.

In most of the cases, the operational HCA output classified regions of graupel prior to the first LMA-indicated flash. Most often this is related to the increase in Z_H over that expected for dry snow aggregates; in other words, more weight is assigned to graupel as Z_H increases to over 35-40 dBz. From an

operational perspective, it appears that a sudden appearance or expansion in the areas classified as graupel should warrant more attention, as conditions are favorable for the development of electrification and possible lightning initiation.

In the 25 October case, there were several regions of HCA-identified graupel that did not produce flashes. These regions may have been electrified but not sufficiently strong to induce a lightning discharge. However, this case did exhibit a polarimetric signature with information about electrification in the cloud preceding a flash (described below). This would generally be useful for lightning potential predictions of such events. Opposed to multiple regions with polarimetric signatures of graupel, no other regions of graupel were identified in other cells near the time of the LMA-detected flashes in the other three thundersnow cases.

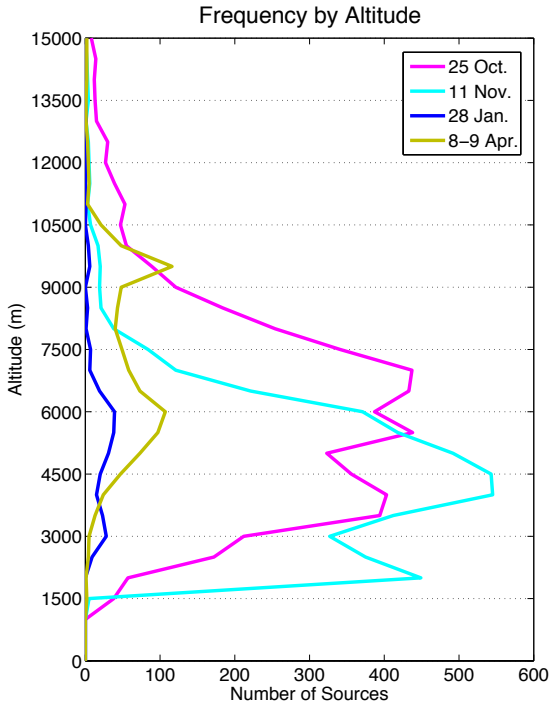

Figure 4: *Source frequency binned by altitude for each of the four cases. Note that the vertical axes do not correspond to each other. LMA sources are thresholded by altitude and $\chi^2<2$. Aircraft tracks have been subjectively identified and removed.*

Lightning activity that occurred during 25 October and 11 November 2012 lasted up to 60 minutes in some cells with a flash rate of up to 5 flashes per minute. Not surprisingly, charge centers were generally at lower altitudes than for summer thunderstorms. Investigating LMA data, most cells for the 25 October case exhibited a typical tripole charge structure with a lower positive charge region followed by a negative charge region and an upper positive charge region. Continental United States (CONUS) lightning detection networks detected some lightning for some of these cells as well. For the 11 November case, charge layers were lower than for 25 October. Analyzing individual flashes from the 11 November case suggests that there was a negative charge region fairly close to the ground centered around 2 km (-10 °C) followed by an upper positive charge region centered at around 4.5 km (-30 °C). Flashes from the 28

January case were all very low with only very few flashes. The 8-9 April case also only exhibited a few flashes but they occurred higher up in altitude. Figure 4 shows the number of VHF sources versus altitude for all four cases. A variety of flash types are found in the variety of storm cells. For example, storm cells from 11 November produced numerous in-cloud discharges as well as negative cloud-to-ground discharges. The latter coincided with the location of mature storm cores. These were also detected by several Continental United States (CONUS) lightning detection networks. Positive cloud-to-ground strikes occurred with decaying cells.

While most flashes from the four cases we investigated were associated with clearly identifiable cells, we found examples where this is not the case. For example, a flash detected by the LMA and a CONUS lightning detection network on 25 October 2012 occurred in the absence of any obvious convective structure in the radar data. Investigating the LMA data from this flash suggests it initiated at low altitude as a negative in-cloud flash and ended with negative cloud-to-ground strokes (Figure 5). Despite not having a clear convective structure apparent in the radar data or large Z_H values (> 35 dBz) that could be indicative of graupel, the 25 October case did exhibit a polarimetric radar signature indicative of electrification in the volume scan preceding the flash (Fig. 6). The cloud was sufficiently strongly electrified that low-inertia ice crystals were oriented at angles off the principal polarization plane axes (i.e., not 0° or 90°). Radars that operate in a mode of simultaneous transmission and reception of H and V polarized waves (such as the WSR-88DPs) produce an artifact when the beam propagates through canted ice crystals. The canted media lead to depolarization of the signal, resulting in radial streaks of positive or negative Z_{DR} (e.g., Ryzhkov and Zrnić 2007; Hubbert et al. 2010; Kumjian 2013c). Such a depolarization streak is evident in the 0.92° PPI of Z_{DR} from KCYS at 0035 UTC (Fig. 6b), about 4 minutes prior to the flash. Note that it is exceedingly unlikely for the negative Z_{DR} streaks to be caused by differential attenuation in this case, as (i) the precipitation was entirely snow at this time, (ii) the WSR-88DP radar operates at S band, at which specific differential attenuation for snow is negligibly small owing to the very small imaginary part of the complex relative permittivity of ice particles, and (iii) maximum Z_H values are rather low, indicating a lack of very large sizes or concentrations of particles necessary to produce attenuation at S band. The streak also moves in time (cf. Figure 6c-f) indicating that it is not caused by anisotropic beam blockage.

Concurrent with the appearance of the depolarization streaks in Z_{DR} were alternating streaks in Φ_{DP}. Φ_{DP}, however, is not currently displayed in the National Weather Service Advanced Weather Interactive Processing System (AWIPS) software. Figure 7 provides an average of radial traces of Z_H, Z_{DR}, and Φ_{DP} through the depolarization streak at 0039 UTC. Note the oscillation of Φ_{DP} as Z_{DR} decreases below 0 dB, coincident with modest Z_H of 20-25 dBz. The increase of Φ_{DP} in a region of modest Z_H and low Z_{DR} also provides important information. Despite larger isotropic particles (presumably aggregates or small rimed particles) dominating the contributions to Z_H and Z_{DR}, pristine anisotropic crystals are also present amongst the aggregates. This is because the fluffy snow aggregates or graupel are invisible to Φ_{DP}. Thus, the combination of each polarimetric variable provides information about a mixture of particles being present simultaneously in the cloud, among which interactions are thought to play a role in charging.

Interestingly, the depolarization streaks persisted for another ~15 minutes after the flash, indicating that the cloud was still electrified, albeit insufficient for a lightning discharge. This example demonstrates that depolarization streaks in Z_{DR} can be useful indicators of electrification, though they themselves do not

necessarily indicate that a lightning strike is imminent.

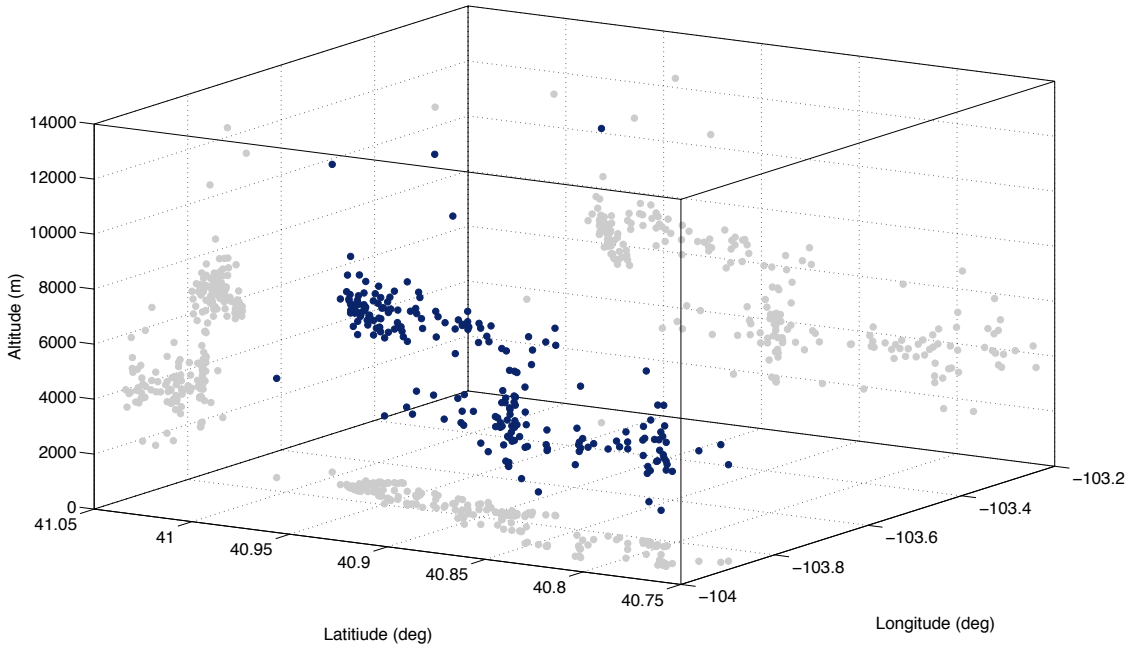

Figure 5: *3D plot of LMA VHF sources, showing a cloud-to-ground flash that occurred on 25 October 2012 in a stratiform region. LMA VHF sources are plotted as a function of latitude, longitude, and altitude (blue markers), with the projections of the flash on each lateral side in gray.*

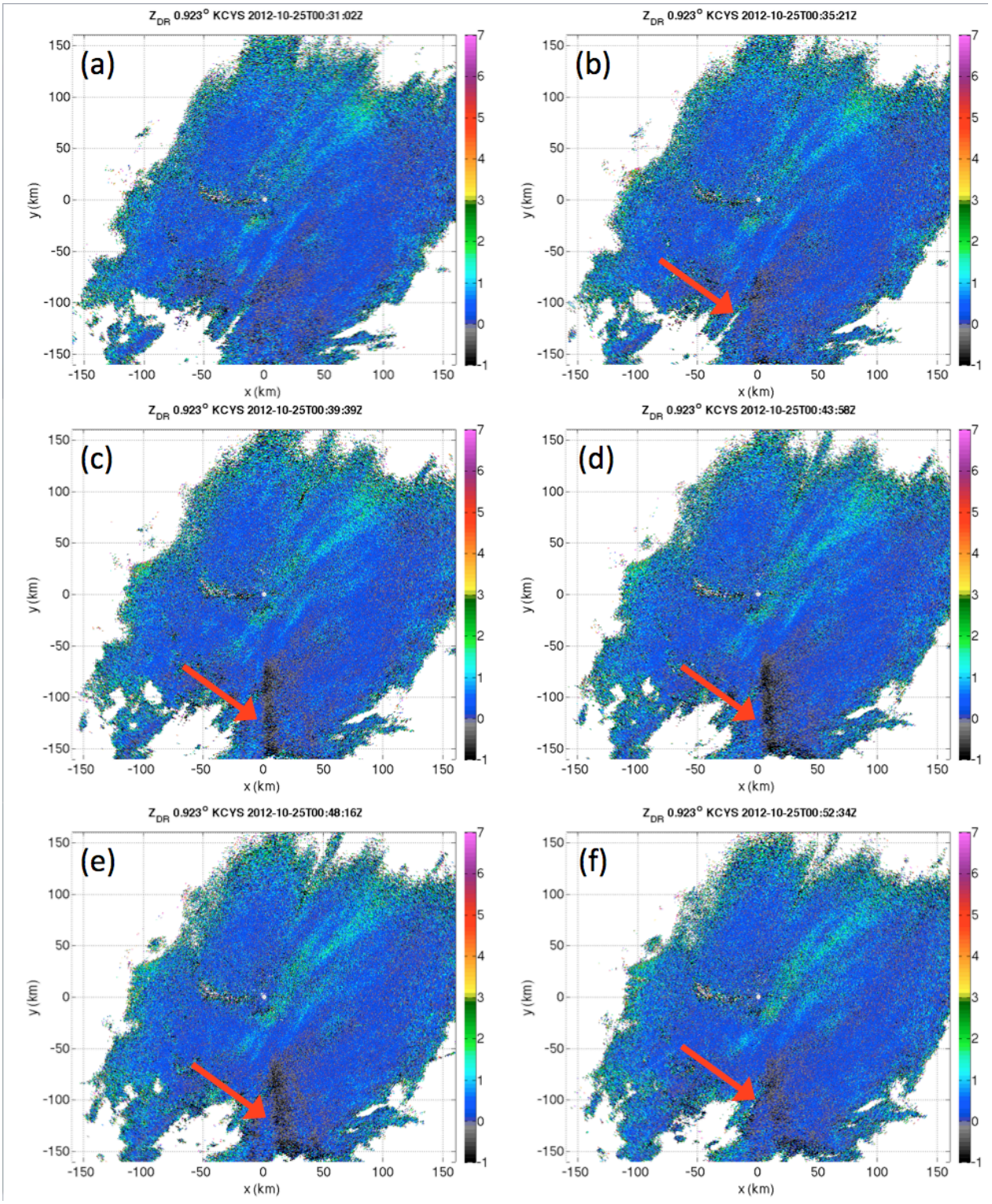

Figure 6: *Consecutive fields of Z_{DR} from the 0.92° PPI scan of KCYS on 25 October 2012. Times shown are (a) 0031 UTC, (b) 0035 UTC, (c) 0039 UTC, (d) 0043 UTC, (e) 0048 UTC, and (f) 0052 UTC. The red arrow points to the location of the observed depolarization streaks.*

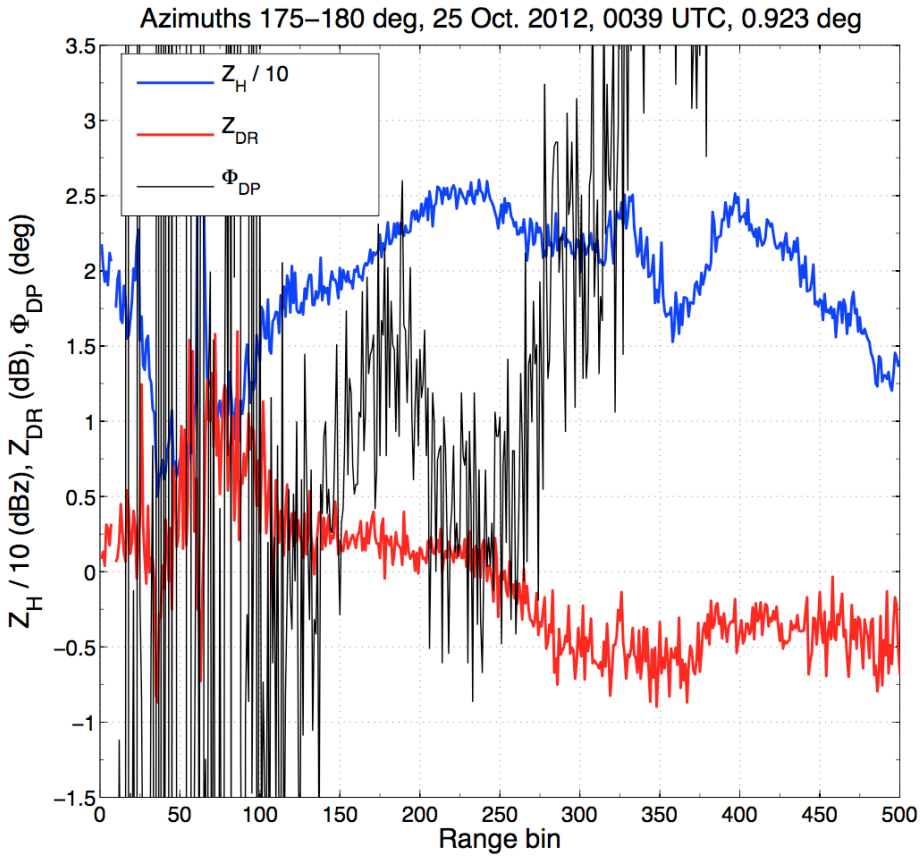

Figure 7: *Traces of azimuthally averaged profiles of Z_H (blue), Z_{DR} (red), and Φ_{DP} (black) through the depolarization streaks. Note that Z_H is divided by 10 for display purposes.*

CONCLUSIONS

The four thundersnow events presented in this study display common features in their synoptic environment, radar presentation, and in the vertical distribution of LMA sources. Each case featured a large-scale environment conducive for ascent, with low-level mesoscale features that provided upslope flow. In particular, the Palmer Divide was found to be a preferred location for electrically active storms. In each case the surface temperature was just under 0 °C.

Though many of the flash events were associated with localized high-Z_H, low-Z_{DR} regions (i.e., presumably convective regions and graupel production), there were several cases of isolated flashes in regions of presumably snow aggregates. In these regions the electric fields are high enough for lightning to occur. In support of the existence of a stronger electric field, in the one case we show above, polarimetric radar data did display a depolarization streak signature prior to the lightning flash.

Compared to previously published climatologies of thundersnow events, the relatively prolific number of events in the 2012-2013 snow season in northern Colorado strongly suggests that thundersnow may be more common than previously thought. Lightning mapping array networks (LMA) allow for detection of events with very low amount of flashes (in particular in-cloud) that may go undetected by CONUS networks.

ACKNOWLEDGMENTS

The National Center for Atmospheric Research (NCAR) is supported by the National Science Foundation (NSF). We would like to thank Jim Dye and Matthias Steiner for valuable discussions on this research. The first author would like to thank the Advanced Study Program at NCAR, which provided support for some of this study.

REFERENCES

Boccippio, D. J., S. J. Goodman, and S. Heckman, 2000: Regional differences in tropical lightning distributions, *J. Appl. Meteorol.*, **39**, 2231-2248.

Bringi, V.N. and V. Chandrasekar, 2001: *Polarimetric Doppler Weather Radar: Principles and Applications*. Cambridge University Press, 636 pp.

Crowe, C., P. Market, B. Pettigrew, C. Melick, and J. Podzimek, 2006: An investigation of thundersnow and deep snow accumulations. *Geophys. Res. Lett.*, **33**, L24812.

Curran, J. T. and A. D. Pearson, 1971: Proximity soundings for thunderstorms with snow. Preprints, *7th Conf. on Severe Local Storms*. Amer. Meteor. Soc., Kansas City, MO, 118-119.

Doviak, R. J., and D. S. Zrnić, 1993: *Doppler Radar and Weather Observations*. Academic Press, 562 pp.

Fukao, S., Y. Maekawa, Y. Sonoi, and F. Yoshino, 1991: Dual polarization radar observation of thunderclouds on the coast of the Sea of Japan in the winter season. *Geophys. Res. Lett.*, **18**, 179-182.

Hubbert, J. C., S. M. Ellis, M. Dixon, and G. Meymaris, 2010: Modeling, error, analysis, and evaluation of dual-polarization variables obtained from simultaneous horizontal and vertical polarization transmit radar. Part II: Experimental data. *J. Atmos. Oceanic Technol.*, **27**, 1599-1607.

Hunter, S. M., S. J. Underwood, R. L. Holle, and T. L. Mote, 2001: Winter lightning and heavy frozen precipitation in the southeast United States. *Wea. Forecasting*, **16**, 478-490.

Kumjian, M. R., 2013a: Principles and applications of dual-polarization weather radar. Part I: Description of the polarimetric radar variables. *J. Operational Meteor.*, **1**(19), 226-242.

Kumjian, M. R., 2013b: Principles and applications of dual-polarization weather radar. Part II: Warm- and cold-season applications. *J. Operational Meteor.*, **1**(20), 243-264.

Kumjian, M. R., 2013c: Principles and applications of dual-polarization weather radar. Part III: Artifacts. *J. Operational Meteor.*, **1**(21), 265-274.

Lang, T. J., L. J. Miller, M. Weisman, S. A. Rutledge, L. J. Baker III, V. N. Bringi, V. Chandrasekar, A. Detwiler, N. Doesken, J. Helsdon, C. Knight, P. Krehbiel, W. A. Lyons, D. MacGorman, E. Rasmussen, W. Rison, W. D. Rust, and R. J. Thomas, 2004: *The severe thunderstorm*

electrification and precipitation study. Bulletin of the American Meteorological Society, **85**(8), 1107 – 1125.

Maekawa, Y., S. Fukao, and F. Yoshino, 1992: Dual polarization radar observations of anomalous wintertime thunderclouds in Japan. *IEEE Trans. Geosci. Remote Sens.*, **30**, 838-844.

Maekawa, Y., S. Fukao, Y. Sonoi, and F. Yoshino, 1993: Distribution of ice particles in wintertime thunderclouds detected by a C band dual polarization radar: A case study. *J. Geophys. Res.*, **98**, 16613-16622.

Market, P. S., C. E. Halcomb, and R. Ebery, 2002: A climatology of thundersnow events over the contiguous United States. *Wea. Forecasting*, **17**, 1290-1295.

Market, P. S., A. M. Oravetz, D. Gaede, E. Bookbinder, A. R. Lupo, C. Melick, L. L. Smith, R. Thomas, and R. Redburn, 2006: Proximity soundings of thundersnow in the central United States. *J. Geophys. Res.*, **111**, D19208.

Pettegrew, B. P., P. S. Market, R. A. Wold, R. L. Holle, and N. W. S. Demetriades, 2009: A case study of severe winter convection in the Midwest. *Wea. Forecasting*, **24**, 121-139.

Ryzhkov, A. V. and D. S. Zrnić, 2007: Depolarization in ice crystals and its effect on radar polarimetric measurements. *J. Atmos. Oceanic Technol.*, **24**, 1256-1267.

Ryzhkov, A.V., T.J. Schuur, D.W. Burgess, P.L. Heinselman, S.E. Giangrande, and D.S. Zrnić, 2005: The joint polarization experiment. *Bull. Amer. Meteor. Soc.*, **86**, 809-824.

Schultz, D. M., 1999: Lake-effect snowstorms in northern Utah and western New York with and without lightning. *Wea. Forecasting,* **14**, 1023-1031.

Schultz, D. M. and J. Vavrek, 2009: An overview of thundersnow. *Weather*, **64**, 274-277.

Straka, J.M., D.S. Zrnić, and A.V. Ryzhkov, 2000: Bulk hydrometeor classification and quantification using polarimetric radar data: synthesis of relations. *J Appl. Meteor.*, **39**, 1341-1372.

Stuart, N., 2001: Multi-dimensional analysis of an extreme thundersnow event during the 30 December 2000 snowstorm. Preprints, *18th Conf. on Weather Analysis and Forecasting*, Ft. Lauderdale, FL, Amer. Meteor. Soc., 223-226.

Thomas, R., P. R. Krehbiel, W. Rison, S. J. Hunyady, W. P. Winn, T. Hamlin, and J. Harlin, 2004: Accuracy of the lightning mapping array. *J. Geophys. Res.*, **109**, D14207, doi:10.1029/2004JD004549.

Zrnić, D.S. and A.V. Ryzhkov, 1999: Polarimetry for weather surveillance radars. *Bull. Amer. Meteor. Soc.*, **80**, 389-406.